

LIGHT CURVES OF SWIFT GAMMA RAY BURSTS

Paolo Cea

*Dipartimento Interateneo di Fisica, Università di Bari, Via G. Amendola 173, I-70126 Bari
and*

INFN - Sezione di Bari, Via G. Amendola 173, I-70126 Bari

Paolo.Cea@ba.infn.it

ABSTRACT

Recent observations from the Swift gamma-ray burst mission indicate that a fraction of gamma ray bursts are characterized by a canonical behaviour of the X-ray afterglows. We present an effective theory which allows us to account for X-ray light curves of both (short - long) gamma ray bursts and X-ray rich flashes. We propose that gamma ray bursts originate from massive magnetic powered pulsars.

Subject headings: gamma-rays: bursts

1. INTRODUCTION

The unique capability of the Swift satellite has yielded the discovery of interesting new properties of short and long gamma ray burst (GRB) X-ray afterglows. Indeed, recent observations have provided new informations on the early behavior ($t < 10^3 - 10^4$ sec) of the X-ray light curves of gamma ray bursts. These early time afterglow observations revealed that (Chincarini 2005; Nousek et al. 2006; O'Brien et al. 2006) a fraction of bursts have a generic shape consisting of three distinct segments: an initial very steep decline with time, a subsequent very shallow decay, and a final steepening (for a recent review, see Piran 2005, Meszaros 2006). This canonical behaviour of the X-ray afterglows of gamma ray bursts is challenging the standard relativistic fireball model, leading to several alternative models (for a recent review of some of the current theoretical interpretations, see Mészáros 2006 and references therein).

In order to determine the nature of both short and long gamma ray bursts, more detailed theoretical modelling is needed to establish a clearer picture of the mechanism. In particular, it is important to have at disposal an unified, quantitative description of the X-ray afterglow

light curves.

The main purpose of this paper is to present an effective theory which allows us to account for X-ray light curves of both gamma ray bursts and X-ray rich flashes (XRF). In a recent paper (Cea 2006) we set up a quite general approach to cope with light curves from anomalous X-ray pulsars (AXP) and soft gamma-ray repeaters (SGR). Indeed, we find that the canonical light curve of the X-ray afterglows is very similar to the light curve after the June 18, 2002 giant burst from AXP 1E 2259+586 (Woods et al. 2004). This suggests that our approach can be extended also to gamma ray bursts.

The plan of the paper is as follows. In Sect. 2 we briefly review the general formalism presented in Cea (2006) to cope with light curves. After that, in Sect. 2.1 through 2.12 we carefully compare our theory with the several gamma ray burst light curves. In Sect. 3 we propose that gamma ray bursts originate from massive magnetic powered pulsars, namely pulsars with super strong dipolar magnetic field and mass $M \sim 10 M_{\odot}$. Finally, we draw our conclusions in Sect. 4.

2. LIGHT CURVES

Gamma ray bursts may be characterized by some mechanism which dissipates injected energy in a compact region. As a consequence the observed luminosity is time-dependent. In this section, following Cea (2006), we briefly discuss an effective description that allows us to determine the light curves, i.e. the time dependence of the luminosity. After that, we shall compare our approach with several light curves of Swift gamma ray bursts.

In general, irrespective of the details of the dissipation process, the dissipated energy leads to the luminosity $L(t) = -\frac{dE(t)}{dt}$. Actually, the precise behavior of $L(t)$ is determined once the dissipation mechanisms are known. However, we may accurately reproduce the time variation of $L(t)$ without precise knowledge of the microscopic dissipative mechanisms. Indeed, on general grounds we expect that the dissipated energy is given by:

$$L(t) = -\frac{dE(t)}{dt} = \kappa(t) E^{\eta} , \quad \eta \leq 1 , \quad (1)$$

where η is the efficiency coefficient. For an ideal system, where the initial injected energy is huge, the linear regime where $\eta = 1$ is appropriate. Moreover, we may safely assume that $\kappa(t) \simeq \kappa_0$ constant. Thus we get:

$$L(t) = -\frac{dE(t)}{dt} \simeq \kappa_0 E . \quad (2)$$

It is then straightforward to solve Eq. (2):

$$E(t) = E_0 \exp\left(-\frac{t}{\tau_0}\right) , \quad L(t) = L_0 \exp\left(-\frac{t}{\tau_0}\right) , \quad (3)$$

$$L_0 = \frac{E_0}{\tau_0} , \quad \tau_0 = \frac{1}{\kappa_0} .$$

Note that the dissipation time $\tau_0 = \frac{1}{\kappa_0}$ encodes all the physical information on the microscopic dissipative phenomena. Since the injected energy is finite, the dissipation of energy degrades with the decrease in the available energy. Thus, the relevant equation is Eq. (1) with $\eta < 1$. In this case, by solving Eq. (1) we find:

$$L(t) = L_0 \left(1 - \frac{t}{t_{dis}} \right)^{\frac{\eta}{1-\eta}} , \quad (4)$$

where we have introduced the dissipation time:

$$t_{dis} = \frac{1}{\kappa_0} \frac{E_0^{1-\eta}}{1-\eta} . \quad (5)$$

Then, we see that the time evolution of the luminosity is linear up to some time t_{break} , and after that we have a break from the linear regime $\eta = 1$ to a non linear regime with $\eta < 1$. If we indicate the total dissipation time by t_{dis} , we get:

$$\begin{aligned} L(t) &= L_0 \exp\left(-\frac{t}{\tau_0}\right) , & 0 < t < t_{break} , \\ L(t) &= L(t_{break}) \left(1 - \frac{t - t_{break}}{t_{dis} - t_{break}} \right)^{\frac{\eta}{1-\eta}} , & t_{break} < t < t_{dis} . \end{aligned} \quad (6)$$

Equation (6) is relevant for light curves where there is a huge amount of energy to be dissipated.

Several observations indicate that after a giant burst there are smaller and more recurrent bursts. According to our approach, we may think about these small bursts as similar to the seismic activity following a giant earthquake (for statistical similarities between bursts and earthquakes, see Cheng et al. 1995). These seismic bursts are characterized by very different light curves from the giant burst light curves.

During these seismic bursts there is an almost continuous injection of energy, which tends to sustain an almost constant luminosity. This corresponds to an effective κ in Eq. (1) which decreases smoothly with time. The simplest choice is:

$$\kappa(t) = \frac{\kappa_0}{1 + \kappa_1 t} . \quad (7)$$

Inserting this into Eq. (1) and integrating, we get:

$$E(t) = \left[E_0^{1-\eta} - (1-\eta) \frac{\kappa_0}{\kappa_1} \ln(1 + \kappa_1 t) \right]^{\frac{\eta}{1-\eta}} , \quad (8)$$

so that the luminosity is:

$$L(t) = \frac{L_0}{(1 + \kappa_1 t)^\eta} \left[1 - (1 - \eta) \frac{\kappa_0}{\kappa_1 E_0^{1-\eta}} \ln(1 + \kappa_1 t) \right]^{\frac{\eta}{1-\eta}} . \quad (9)$$

After defining the dissipation time as

$$\ln(1 + \kappa_1 \tau_{dis}) = \frac{\kappa_1}{\kappa_0} \frac{E_0^{1-\eta}}{1 - \eta} , \quad (10)$$

we rewrite Eq. (9) as

$$L(t) = \frac{L_0}{(1 + \kappa_1 t)^\eta} \left[1 - \frac{\ln(1 + \kappa_1 t)}{\ln(1 + \kappa_1 \tau_{dis})} \right]^{\frac{\eta}{1-\eta}} . \quad (11)$$

Note that the light curve in Eq. (11) depends on two characteristic time constants $\frac{1}{\kappa_1}$ and τ_{dis} . We see that $\kappa_1 \tau_{dis}$, which is roughly the number of small bursts that occurred in the given event, gives an estimation of the seismic burst intensity. Moreover, since during the seismic bursts the injected energy is much smaller than in giant bursts, we expect values of η which are lower with respect to typical values in giant bursts.

As we alluded in the Introduction, the canonical light curves of the X-ray afterglows are very similar to the light curve after the 2002 June 18 giant burst from AXP 1E 2259+586. In Cea (2006) we were able to accurately reproduce the puzzling light curve of the June 2002 burst by assuming that AXP 1E 2259+586 has undergone a giant burst, and soon after has entered into intense seismic burst activity. Accordingly, we may parameterize the X-ray afterglow light curves of gamma ray bursts as:

$$L_{GRB}(t) = L_G(t) + L_S(t) , \quad (12)$$

where, since there are no available data during the first stage of the outbursts, we have for the giant burst's contribution:

$$L_G(t) = L_G(0) \left(1 - \frac{t}{t_{diss}} \right)^{\frac{\eta_G}{1-\eta_G}} , \quad 0 < t < t_{diss} , \quad (13)$$

while $L_S(t)$ is given by:

$$L_S(t) = \frac{L_S(0)}{(1 + \kappa t)^{\eta_S}} \left[1 - \frac{\ln(1 + \kappa t)}{\ln(1 + \kappa \tau_{diss})} \right]^{\frac{\eta_S}{1-\eta_S}} , \quad 0 < t < \tau_{diss} . \quad (14)$$

Note that, unlike the anomalous X-ray pulsars and soft gamma-ray repeaters, we do not need to take care of the quiescent flux since the gamma ray burst sources are at cosmological

distances.

In the following Sections we select a collection of GRBs with the aim to illustrate the variety of displayed light curves. In general, we reproduce the data of light curves from the original figures. For this reason, we display the light curves with the same time intervals as in the original figures. So that, lacking the precise values of data the best fits to our light curves are only indicative. In view of this, a quantitative comparison with different models is not possible. The unique exception is GRB 050801 where the data was taken from Table 1 in Rykoff et al. (2006). In that case (see Sect. 2.4) we indicate the reduced chisquare.

2.1. GRB 050315

On 2005 March 15 the Swift Burst Alert Telescope (BAT) triggered and located on-board GRB 050315 (Vaughan et al. 2006). After about 80 *sec* the Swift X-ray Telescope (XRT) began observations until about 10 *days*, providing one of the best-sampled X-ray light curves of a gamma ray burst afterglow.

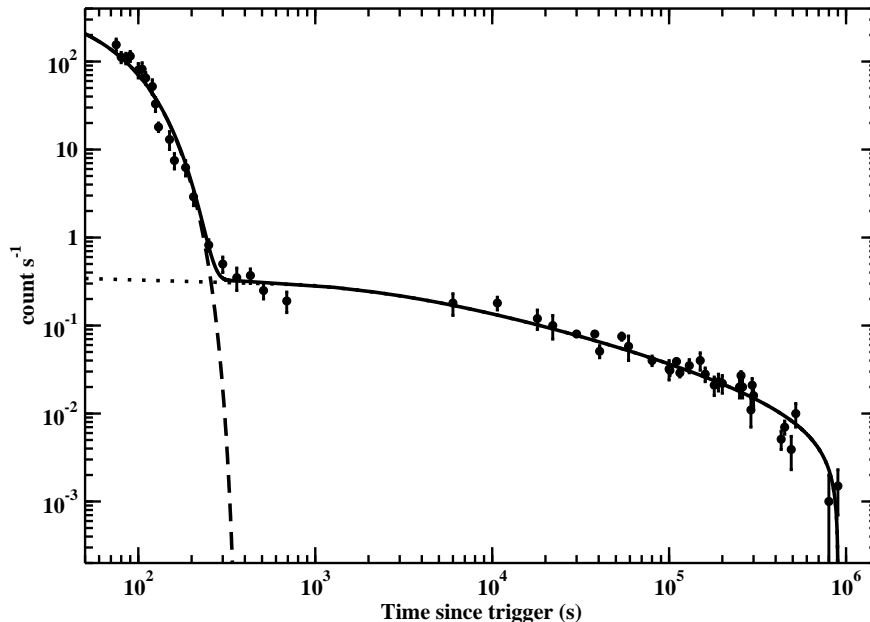


Fig. 1.— Light curve of GRB 050315 in the 0.2 – 5 *keV* band. The data was extracted from Fig. 5 in Vaughan et al. (2006). The full line is our light curve Eq. (12); the dashed and dotted lines are Eq. (13) and Eq. (14) respectively, with parameters in Eq. (15).

In Fig.1 we display the light curve of GRB 050315 in the $0.2 - 5 \text{ keV}$ band. The data was extracted from Fig. 5 in Vaughan et al.(2006).

A tentative fit to the X-ray light curve within the standard relativistic fireball model has been proposed in Granot et al. (2006) using a two-component jet model. An alternative description of the light curve of GRB 050315 within the cannonball model is presented in Dado & De Rujula (2005).

We fitted the data to our light curve Eq. (12). Indeed, we find a rather good description of the data with the following parameters (see Fig. 1):

$$\begin{aligned} L_G(0) &\simeq 5.2 \cdot 10^2 \frac{\text{count}}{\text{sec}} , & \eta_G &\simeq 0.867 , & t_{diss} &\simeq 380 \text{ sec} \\ L_S(0) &\simeq 0.35 \frac{\text{count}}{\text{sec}} , & \eta_S &\simeq 0.4 , & \tau_{diss} &\simeq 9.0 \cdot 10^5 \text{ sec} , & \kappa &\simeq 5.0 \cdot 10^4 \text{ sec}^{-1} . \end{aligned} \quad (15)$$

A few comments are in order. As discussed in the Sect. 2, since we lack the precise values of data, a quantitative comparison of our light curve with data is not possible. Nevertheless, Fig. 1 shows that the agreement with data is rather good. Moreover, our efficiency exponents η_G and η_S are consistent with the values found in giant bursts from anomalous X-ray pulsars and soft gamma-ray repeaters (Cea 2006). Note that, as expected, we have $\eta_S < \eta_G$.

2.2. GRB 050319

Swift discovered GRB 050319 with the Burst Alert Telescope and began observing after 225 s after the burst onset (Cusumano et al. 2006).

The X-ray afterglow was monitored by the XRT up to 28 days after the burst. In Fig. 2 we display the X-ray light curve in the $0.2 - 10 \text{ keV}$ band. The data are extracted from Fig. 2 in Cusumano et al. (2006). Note that the light curve in the early stage of the outflow has been obtained extrapolating the BAT light curve in the XRT band by using the the best-fit spectral model (Cusumano et al. 2006).

An adequate description of the XRT light curve of GRB 050319 within the cannonball model is presented in Dado & De Rujula (2005). However, we note that the extrapolation of the best-fit light curve towards the first stage of the outburst overestimates the observed flux by orders of magnitude. On the other hand, we may easily account for the observed flux decay by our light curve. Indeed, in Fig. 2 we compare our light curve Eq. (12) with observational data. The agreement is quite satisfying, even during the early-time of the outburst, if we take:

$$\begin{aligned} L_G(0) &\simeq 8.5 \cdot 10^{-8} \frac{\text{erg}}{\text{cm}^2 \text{ sec}} , & \eta_G &\simeq 0.867 , & t_{diss} &\simeq 410 \text{ sec} \\ L_S(0) &\simeq 5.5 \cdot 10^{-9} \frac{\text{erg}}{\text{cm}^2 \text{ sec}} , & \eta_S &\simeq 0.45 , & \tau_{diss} &\simeq 7.5 \cdot 10^5 \text{ sec} , & \kappa &\simeq 10 \text{ sec}^{-1} . \end{aligned} \quad (16)$$

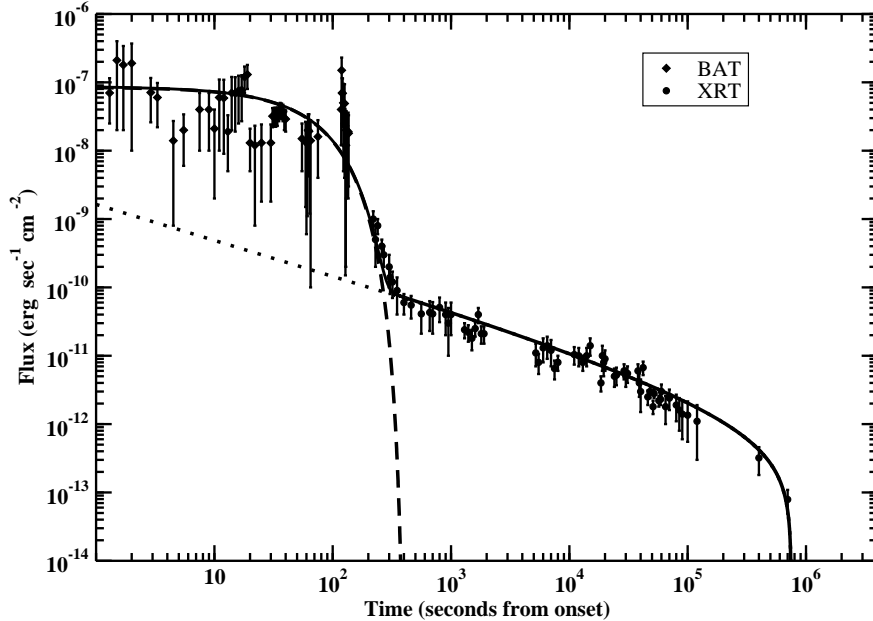


Fig. 2.— XRT light curve of GRB 050319 in the $0.2 - 10 \text{ keV}$ band. The data was extracted from Fig. 2 in Cusumano et al. (2006). The BAT light curve was obtained by extrapolating the BAT count rate into the XRT energy band with the best-fit spectral model (Cusumano et al. 2006). The full line is our light curve Eq. (12); the dashed and dotted lines are Eq. (13) and Eq. (14) respectively, with parameters in Eq. (16).

2.3. XRF 050406

On 2005 April 6 BAT triggered on GRB 050406 (Romano et al. 2006a). The gamma-ray characteristics of this burst, namely the softness of the observed spectrum and the absence of significant emission above $\sim 50 \text{ keV}$, classify the burst as an X-ray flash (XRF 050406).

In Fig. 3 we display the time decay of the flux. The data was taken from Fig. 2 in Romano et al. (2006a). We fit our light curve Eq. (12) to the available data. Indeed, we find that our light curve, with parameters given by:

$$\begin{aligned}
 L_G(0) &\simeq 1.75 \frac{\text{count}}{\text{sec}} , \quad \eta_G \simeq 0.839 , \quad t_{diss} \simeq 1.5 \cdot 10^3 \text{ sec} \\
 L_S(0) &\simeq 0.15 \frac{\text{count}}{\text{sec}} , \quad \eta_S \simeq 0.40 , \quad \tau_{diss} \simeq 8.0 \cdot 10^6 \text{ sec} , \quad \kappa \simeq 0.2 \text{ sec}^{-1} ,
 \end{aligned}
 \tag{17}$$

allows quite a satisfying description of the decline of the flux (see Fig. 3). Note that in the fit we exclude the bump at $t \sim 200 \text{ sec}$. For completeness, we also display in Fig. 3 the phenomenological best-fit broken power law (Romano et al. 2006a). It is worthwhile to observe that the bump in the flux at $t \sim 200 \text{ sec}$ is similar to the April 18, 2001 flare from

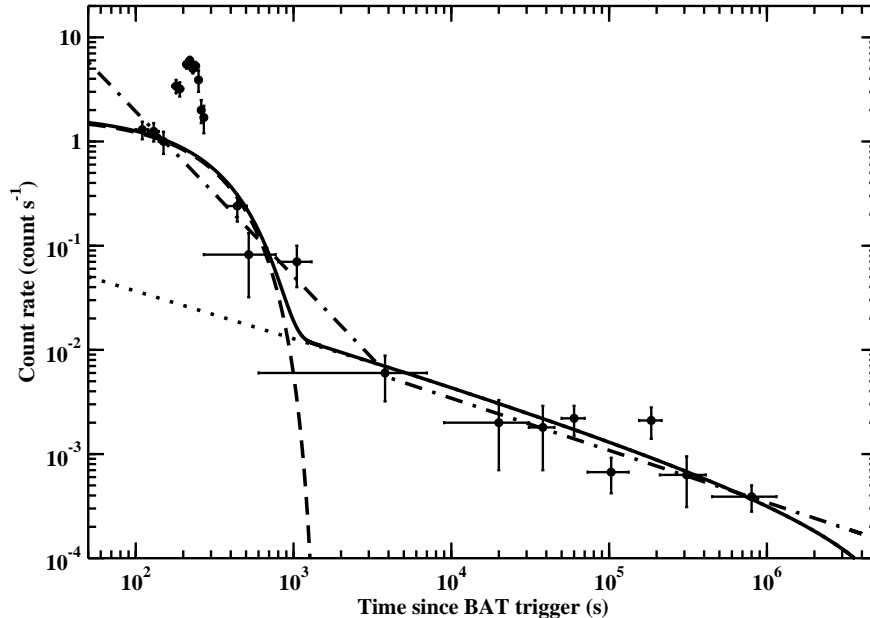


Fig. 3.— X-ray light curve of XRF 050406 in the $0.2 - 10 \text{ keV}$ energy band. The data was extracted from Fig. 2 in Romano et al. (2006a). The dot-dashed line is the broken power-law best fit (Romano et al. 2006a). The full line is our light curve Eq. (12); the dashed and dotted lines are Eq. (13) and Eq. (14) respectively, with parameters in Eq. (17).

SGR 1900+14 (Feroci et al. 2003). Indeed, within our approach we believe that the bump in the flux could naturally be explained as fluctuations in the intense burst activity (see Sect. 5.2 in Cea 2006).

2.4. GRB 050801

The Swift XRT obtained observations starting at 69 seconds after the burst onset of GRB 050801 (Rykoff et al. 2006). In Fig. 4 we display the flux decay, where the data has been extracted from Table 1 in Rykoff et al. (2006).

In this case we are able to best fit our light curve Eq. (12) to the available data. Since the observations start from $t > 74 \text{ s}$, we perform the fit of data to the seismic burst light curve $F_S(t)$, Eq. (14). To get a sensible fit we fixed the dissipation time to $\tau_{diss} = 2.0 \cdot 10^6 \text{ s}$ and $\kappa = 10^{-2} \text{ s}^{-1}$. The best fit of our light curve to data gives:

$$L_S(0) = (27.4 \pm 7.2) \cdot 10^{-11} \frac{\text{erg}}{\text{cm}^2 \text{ sec}}, \quad \eta_S = 0.748 \pm 0.026, \quad (18)$$

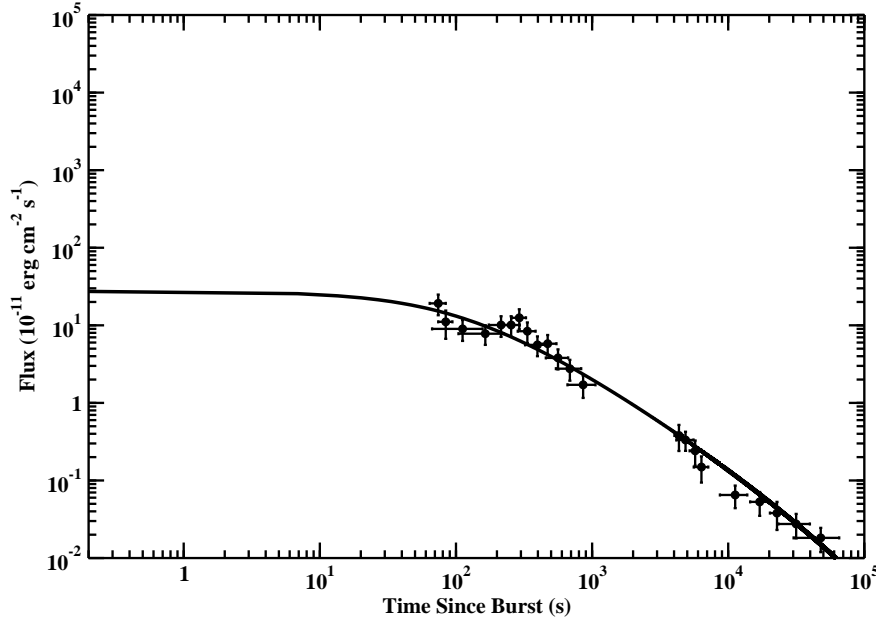


Fig. 4.— X-ray light curve of GRB 050801. The data was taken from Table 1 in Rykoff et al. (2006). The full line is our best-fit light curve Eq. (14) with parameters in Eq. (18).

with a reduced $\chi^2/dof \simeq 0.93$. In Fig. 4 we compare our best-fitted light curve with data. We see that our theory allows a satisfying description of the light curve of GRB 050801. On the other hand, it is difficult to explain the peculiar behaviour of the light curve with standard models of early afterglow emission without assuming that there is continuous late time injection of energy into the afterglow (Rykoff et al. 2006).

2.5. GRB 051221A

GRB 051221A was detected by the Swift BAT on 2005 December 21. The Swift XRT observations began 88 seconds after the BAT trigger. The late X-ray afterglow of GRB 051221A has been also observed by the Chandra ACIS-S instrument. The combined X-ray light curve, displayed in Fig. 5, was extracted from Fig. 2 in Burrows et al. (2006).

From Fig. 5, we see that the combined X-ray light curve is similar to those commonly observed in long gamma ray bursts. However, we find that this peculiar light curve could be interpreted within our approach as the superimposition of two different seismic bursts. Accordingly, we may account for the X-ray afterglow light curve of GRB 051221A by:

$$L_{GRB}(t) = L_{S_1}(t) + L_{S_2}(t) \quad . \quad (19)$$

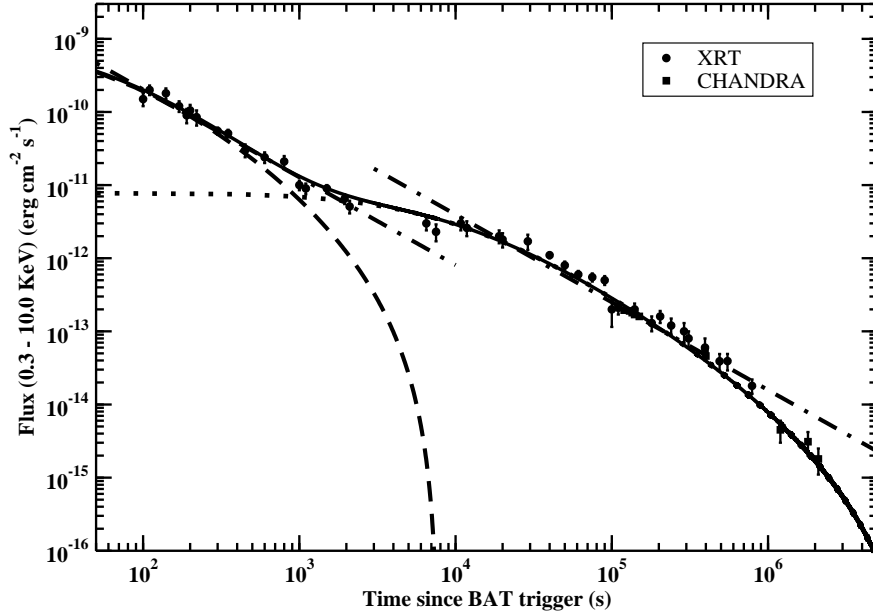


Fig. 5.— Combined XRT and CHANDRA light curve of the afterglow of GRB 051221A. The data was extracted from Fig. 2 in Burrows et al. (2006). The dot-dashed lines are the phenomenological power law fits $t^{-1.20}$. The full line is our light curve Eq. (19), the dashed line is $L_{S_1}(t)$, and the dotted line is $L_{S_2}(t)$.

Indeed, we find that our light curve Eq. (19) allows a rather good description of the data once the parameters are:

$$L_{S_1}(0) \simeq 9.8 \cdot 10^{-10} \frac{erg}{cm^2 sec}, \eta_{S_1} \simeq 0.74, \tau_{diss_1} \simeq 7.8 \cdot 10^3 sec, \kappa_1 \simeq 2.3 \cdot 10^{-2} sec^{-1} \quad (20)$$

$$L_{S_2}(0) \simeq 8.0 \cdot 10^{-12} \frac{erg}{cm^2 sec}, \eta_{S_2} \simeq 0.40, \tau_{diss_2} \simeq 1.0 \cdot 10^7 sec, \kappa_2 \simeq 1.4 \cdot 10^{-4} sec^{-1}.$$

It is worth mentioning that the data displayed in Fig. 5 start at $t > 10^2 sec$. So that we cannot reliably determine the eventual giant burst contribution. On the other hand, this peculiar light curve is well described by two different seismic bursts, much like the intense burst activity in anomalous X-ray pulsars and soft gamma-ray repeaters. Note that the phenomenological power law fits overestimate the light curve for $t > 10^6 sec$.

2.6. GRB 050505

On 2005 May 5 the Swift BAT triggered GRB 050505. The X-ray telescope XRT began taking data about 47 minutes after the burst trigger. In Fig. 5 we report the combined XRT and BAT light curve of the afterglow of GRB 050505. The data was extracted from Fig. 5

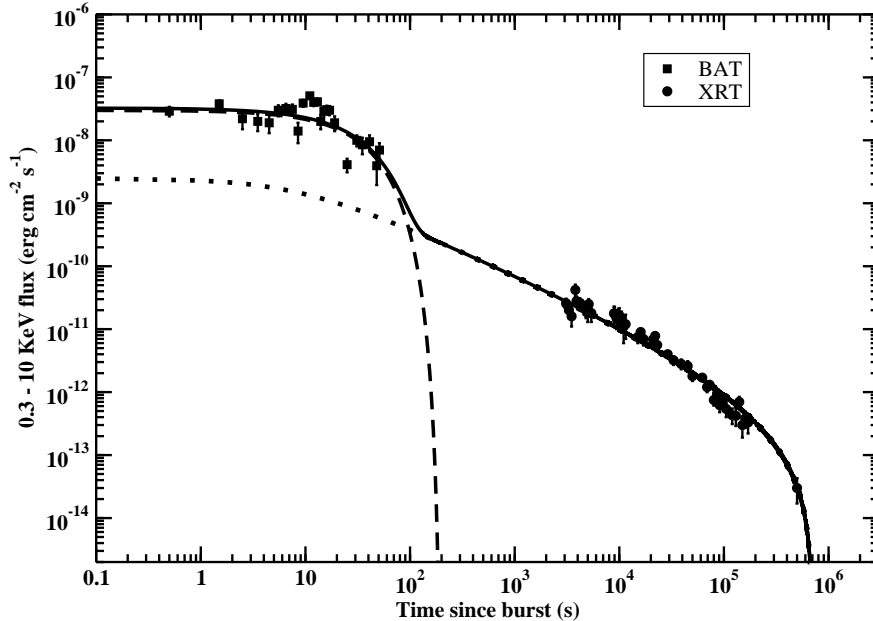


Fig. 6.— The combined BAT-XRT flux light curve of GRB 050505, extrapolated into the 0.3 – 10.0 keV range. The data was extracted from Fig. 5 in Hurkett et al. (2006). The full line is our light curve Eq. (12), the dashed line is Eq. (13), and the dotted line is Eq. (14).

in Hurkett et al. (2006). The BAT data were extrapolated into the the XRT band using the best fit power law model derived from the BAT data alone (Hurkett et al. 2006).

Within the standard models of early afterglows, the light curve is modelled by a broken power law. Nevertheless, we find that our light curve, Eq. (12), with parameters given by:

$$\begin{aligned}
 L_G(0) &\simeq 3.0 \cdot 10^{-8} \frac{\text{erg}}{\text{cm}^2 \text{sec}}, & \eta_G &\simeq 0.867, & t_{diss} &\simeq 2.0 \cdot 10^2 \text{sec} \\
 L_S(0) &\simeq 2.5 \cdot 10^{-9} \frac{\text{erg}}{\text{cm}^2 \text{sec}}, & \eta_S &\simeq 0.58, & \tau_{diss} &\simeq 7.0 \cdot 10^5 \text{sec}, & \kappa &\simeq 0.13 \text{sec}^{-1},
 \end{aligned}
 \tag{21}$$

is able to describe quite well the X-ray afterglow (see Fig. 6).

2.7. GRB 050713A

In Fig. 7 we report the combined XRT and XMM-Newton light curve of the afterglow of GRB 050713A. The data was extracted from Fig. 7 in Morris et al. (2006). The dot-dashed line is the broken-power law best fit of the combined X-ray light curve (Morris et al. 2006).

Within our approach we may reproduce the X-ray afterglow of GRB 050713A by our Eq. (12). However, since the giant burst contribution to the light curve $L_G(t)$ lasts up to

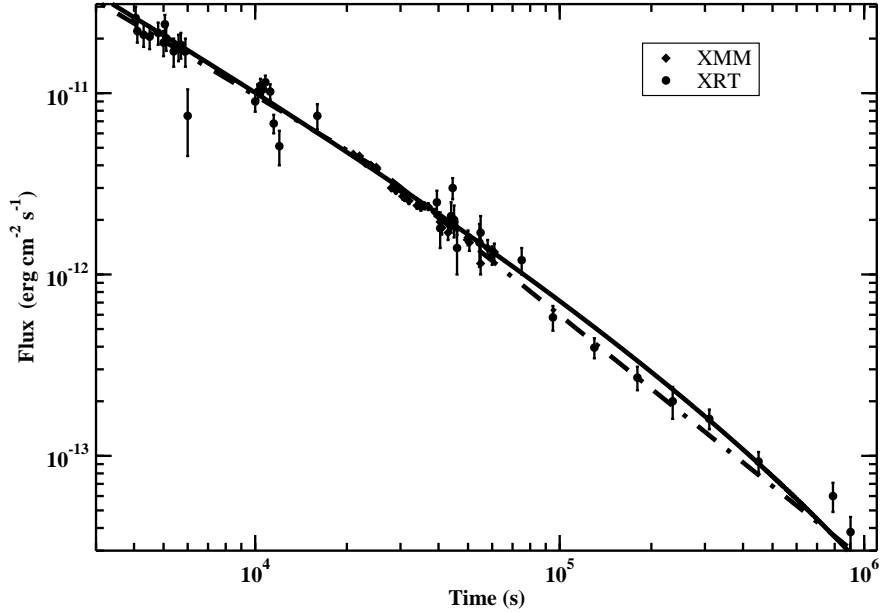


Fig. 7.— Joint Swift XRT and XMM-Newton light curve of the afterglow of GRB 050713A. The data was extracted from Fig. 7 in Morris et al. (2006). The dot-dashed line is the best-fit broken power-law ((Morris et al. 2006)). The full line is our light curve Eq. (22) with parameters in Eq. (23).

$t \sim 10^2 - 10^3 \text{ sec}$, we need to consider only $L_S(t)$. So that we are lead to:

$$L_{GRB}(t) = L_S(t) \quad . \quad (22)$$

Indeed, even in this case our light curve, with parameters fixed to:

$$L_S(0) \simeq 5.5 \cdot 10^{-9} \frac{\text{erg}}{\text{cm}^2 \text{ sec}}, \quad \eta_S \simeq 0.71, \quad \kappa \simeq 7.0 \cdot 10^{-2} \text{ sec}^{-1}, \quad \tau_{diss} \simeq 9.0 \cdot 10^6 \text{ sec}, \quad (23)$$

reproduces quite accurately the phenomenological broken-power law best fit (see Fig. 7).

2.8. GRB 051210

GRB 051210 triggered the Swift BAT on 2005 December 12. The burst was classified as short gamma ray burst. In Fig. 2 in La Parola et al. (2006) it is presented the XRT light curve decay of GRB 051210. The BAT light curve was extrapolated into the $0.2 - 10 \text{ keV}$ band by converting the BAT count rate with the factor derived from the BAT spectral parameters.

In Fig. 8 we report the combined BAT and XRT light curve of the afterglow of GRB

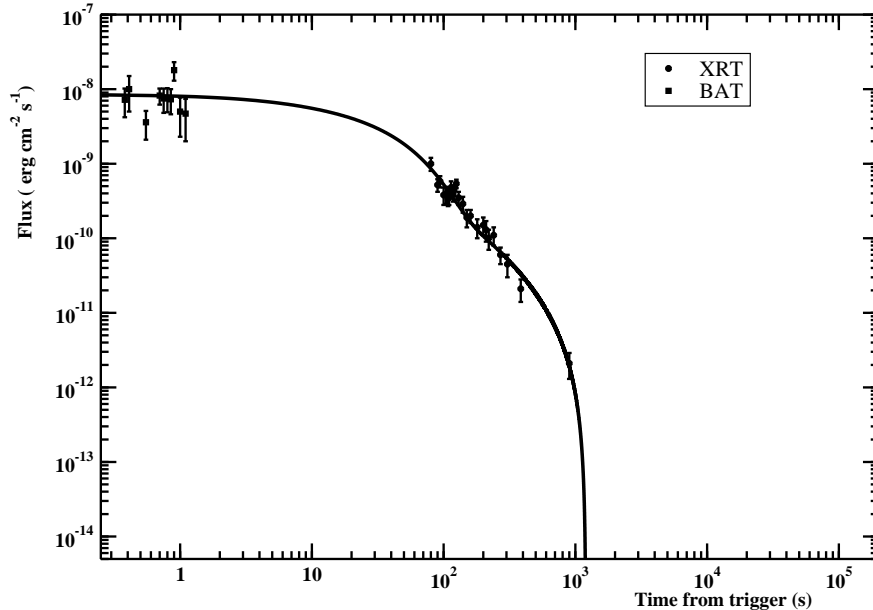


Fig. 8.— XRT light curve of GRB 051210. The data was extracted from Fig. 2 in La Parola et al. (2006). The BAT light curve was extrapolated into the XRT energy band with the best-fit spectral model (La Parola et al 2006). The full line is our light curve Eq. (12) with parameters in Eq. (24).

051210. The data was extracted from Fig. 2 in La Parola et al. (2006). In Fig. 8 we also display our best fit light curve Eq. (12) with parameters:

$$\begin{aligned}
 L_G(0) &\simeq 4.5 \cdot 10^{-9} \frac{\text{erg}}{\text{cm}^2 \text{sec}} , \quad \eta_G \simeq 0.867 , \quad t_{diss} \simeq 2.8 \cdot 10^2 \text{ sec} \\
 L_S(0) &\simeq 4.0 \cdot 10^{-9} \frac{\text{erg}}{\text{cm}^2 \text{sec}} , \quad \eta_S \simeq 0.63 , \quad \tau_{diss} \simeq 1.2 \cdot 10^3 \text{ sec} , \quad \kappa \simeq 0.1 \text{ sec}^{-1} .
 \end{aligned}
 \tag{24}$$

Even in this case the agreement between our light curve and the data is satisfying.

2.9. GRB 060121

GRB 060121 was detected by HETE-2 on January 21, 2006. Swift performed observations beginning at January 22, 2006 (Levan et al 2006). GRB 060121 was identified as a short and spectrally hard burst.

In Fig. 9 we report the X-ray light curve in the $0.3 - 10.0 \text{ keV}$ band. The data has been extracted from Fig. 1 in Levan et al. (2006). We also display the phenomenological power-law best fit $L(t) \sim t^{-1.18}$ (Levan et al 2006).

Within our approach we may reproduce the X-ray afterglow of GRB 050713A by our

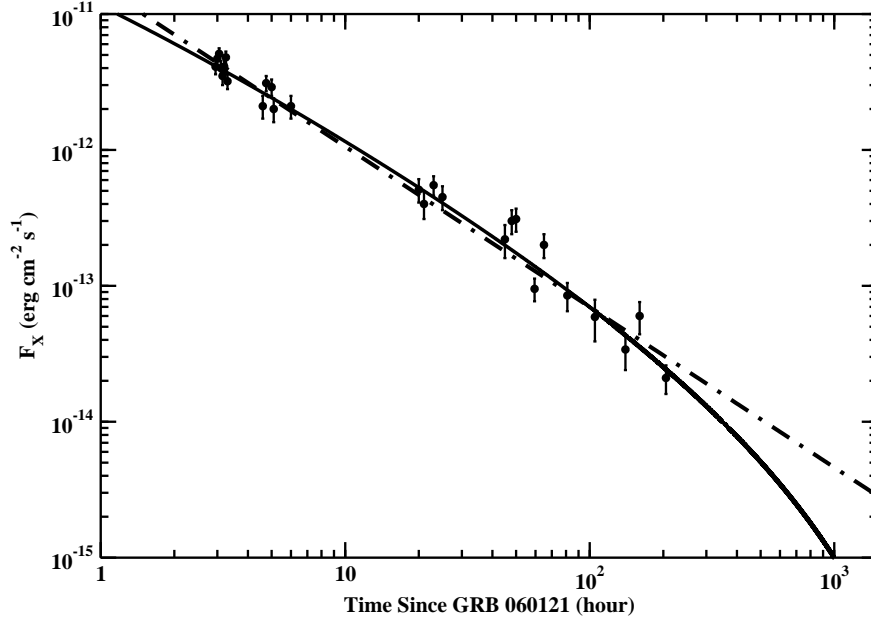


Fig. 9.— X-ray ($0.2 - 10 \text{ keV}$) light curve of GRB 060121. The data was extracted from Fig. 1 in Levan et al. (2006). The dot-dashed line is the phenomenological power-law fit (Levan et al 2006). The full line is our light curve Eq. (22) with parameters in Eq. (25).

Eq. (12). Even in this case we need to consider only the seismic burst contribution $L_S(t)$. Indeed, we find that our Eq. (22) reproduces quite accurately the phenomenological power law best fit with the following parameters (see Fig. 9):

$$L_S(0) \simeq 9.5 \cdot 10^{-11} \frac{\text{erg}}{\text{cm}^2 \text{sec}}, \quad \eta_S \simeq 0.70, \quad \kappa \simeq 8.0 \text{ hour}^{-1}, \quad \tau_{diss} \simeq 3.0 \cdot 10^3 \text{ hour}. \quad (25)$$

2.10. GRB 060124

Swift BAT triggered on a precursor of GRB 060124 on 2006 January 24, about 570 seconds before the main burst. So that GRB 060124 is the first event for which there is a clear detection of both the prompt and the afterglow emission (Romano et al. 2006b).

In Fig. 10 we report the X-ray light curve in the $0.3 - 10.0 \text{ keV}$ band. The data has been extracted from Fig. 9 in Romano et al. (2006b). In Fig. 10 we display our best fit light curve Eq. (12) with parameters:

$$\begin{aligned} L_G(0) &\simeq 5.0 \cdot 10^{-8} \frac{\text{erg}}{\text{cm}^2 \text{sec}}, \quad \eta_G \simeq 0.867, \quad t_{diss} + t_0 \simeq 1.0 \cdot 10^3 \text{ sec} \\ L_S(0) &\simeq 6.5 \cdot 10^{-9} \frac{\text{erg}}{\text{cm}^2 \text{sec}}, \quad \eta_S \simeq 0.60, \quad \tau_{diss} + t_0 \simeq 1.2 \cdot 10^6 \text{ sec}, \quad \kappa \simeq 5.0 \cdot 10^{-2} \text{ sec}^{-1}, \end{aligned} \quad (26)$$

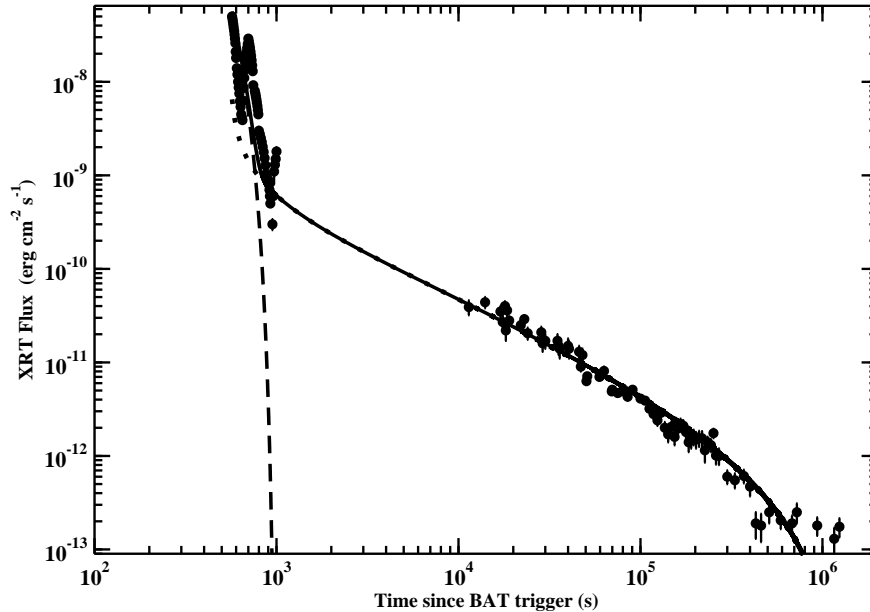


Fig. 10.— X-ray light curve of GRB 060124 in the $0.2 - 10 \text{ keV}$ energy band. The data was extracted from Fig. 9 in Romano et al. (2006b). The full line is our light curve Eq. (12); the dashed and dotted lines are Eq. (13) and Eq. (14) respectively, with parameters given in Eq. (26).

where we assumed that the burst started at $t_0 = 570 \text{ s}$. Note that our light curve interpolates the X-ray peaks at the early stage of the outflow. On the other hand, our light curve mimics quite well the broken power-law best fit to the XRT data (compare our Fig. 10 with Romano et al. (2006b), Fig. 9).

2.11. GRB 060218

GRB 060218 was detected with the BAT instrument on 2006 February 18. XRT began observations 159 seconds after the burst trigger (Campana et al. 2006).

The XRT light curve is shown in Fig. 11. The data was extracted from Fig. 2 in Campana et al. (2006). We try to interpret the XRT light curve with our light curve Eq. (12). The result of our best fit is displayed in Fig. 11. Excluding the data of the bump from $t \sim 200 \text{ sec}$ to $t \sim 3000 \text{ sec}$, the parameters for our best fit light curve are:

$$\begin{aligned}
 L_G(0) &\simeq 4.1 \cdot 10^{-9} \frac{\text{erg}}{\text{cm}^2 \text{sec}}, \quad \eta_G \simeq 0.867, \quad t_{diss} \simeq 1.55 \cdot 10^4 \text{ sec} \\
 L_S(0) &\simeq 8.0 \cdot 10^{-10} \frac{\text{erg}}{\text{cm}^2 \text{sec}}, \quad \eta_S \simeq 0.60, \quad \tau_{diss} \simeq 2.0 \cdot 10^6 \text{ sec}, \quad \kappa \simeq 1.3 \cdot 10^{-2} \text{ sec}^{-1},
 \end{aligned}
 \tag{27}$$

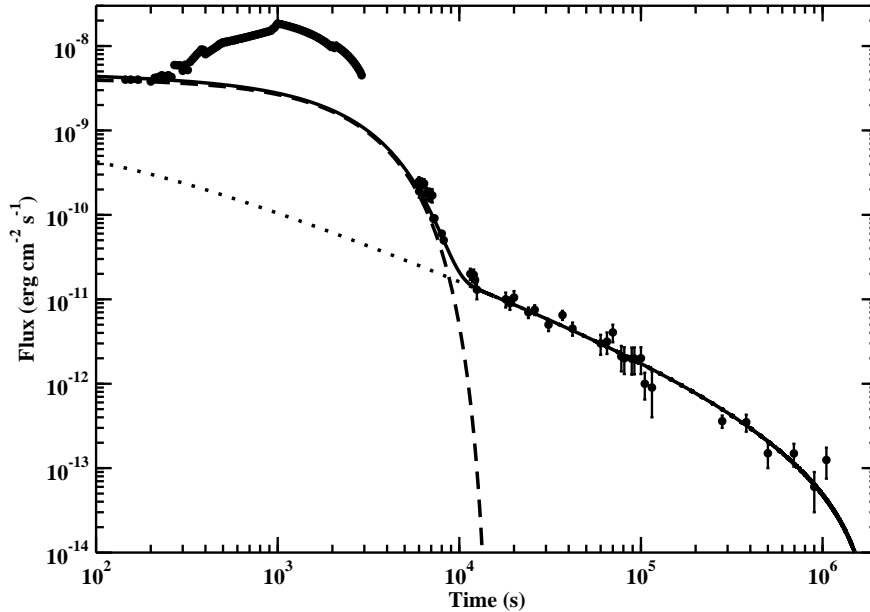


Fig. 11.— XRT light curve ($0.2 - 10 \text{ keV}$) of GRB 060218. The data was extracted from Fig. 2 in Campana et al. (2006). The full line is our light curve Eq. (12); the dashed and dotted lines are Eq. (13) and Eq. (14), respectively.

Indeed, our light curve is able to reproduce quite well the data. However, there is a clear excess in the observed light curve with respect to our light curve in the early-time afterglow. We believe that this excess is due to a component which is not directly related to the burst. Indeed, Campana et al. (2006) pointed out that there was a soft component in the X-ray spectrum, that is present in the XRT starting from 159 s up to about 10^4 s. This soft component could be accounted for by a black body with an increasing emission radius of the order of 10^{12} cm. Moreover, this component is undetected in later XRT observations and it is interpreted as shock break out from a dense wind.

2.12. XRF 050416A

Swift discovered XRF 050416A with the Burst Alert Telescope on 2005 April 16. After about 76 seconds from the burst trigger, XRT began collecting data (Mangano et al 2006). The X-ray light curve was monitored up to 74 days after the onset of the burst. The very soft spectrum of the burst classifies this event as an X-ray flash.

In Fig. 12 we show the combined BAT-XRT light curve of XRF 050416A. The BAT light curve was extrapolated into the $0.2 - 10 \text{ keV}$ energy band assuming two different spectral

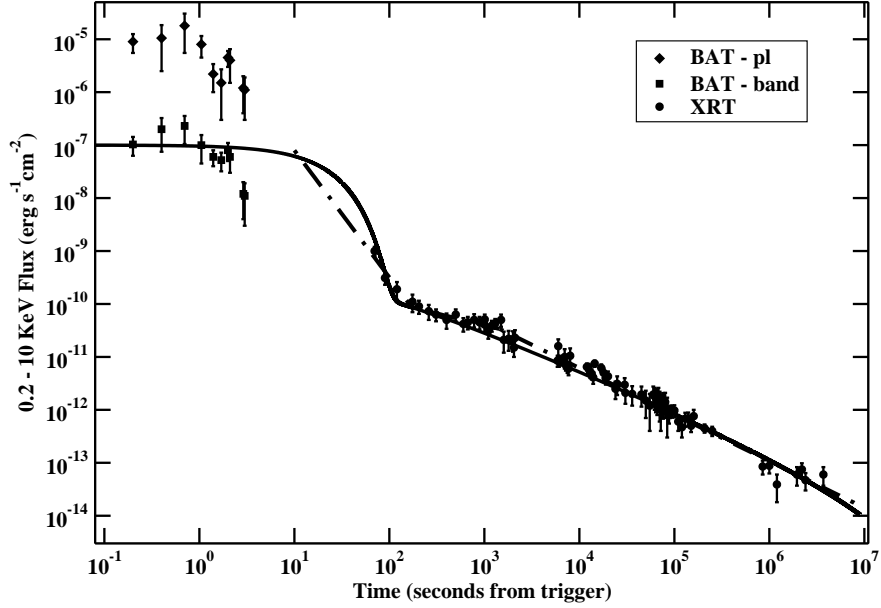


Fig. 12.— BAT and XRT light curves of XRF 050416A. The data was extracted from Fig. 2 in Mangano et al. (2006). The BAT light curve was extrapolated into the XRT energy band with two different spectral models (Mangano et al 2006). The dot-dashed line is the phenomenological broken power-law fit (Mangano et al 2006). The full line is our light curve Eq. (12) with parameters in Eq. (28).

law, the Band best fit model (full squares in Fig. 12) and a single power law best fit model (full diamonds in Fig. 12).

From Fig. 12 we see that the X-ray light curve initially decays very fast and subsequently flattens. It is evident that the XRT light curve decay is not consistent with a single power law. Indeed, Mangano et al. (2006) found that a doubly-broken power law improves considerably the fit of the light curve (dot-dashed line in Fig. 12). On the other hand, we may adequately reproduce the combined BAT-XRT light curve with our light curve Eq. (12). To this end, we assume that the early light curve is described by the BAT data extrapolated with the Band best fit model. By fitting our Eq. (12) to the data, we find:

$$\begin{aligned}
 L_G(0) &\simeq 1.0 \cdot 10^{-7} \frac{\text{erg}}{\text{cm}^2 \text{sec}}, \quad \eta_G \simeq 0.895, \quad t_{diss} \simeq 1.8 \cdot 10^2 \text{ sec} \\
 L_S(0) &\simeq 2.5 \cdot 10^{-10} \frac{\text{erg}}{\text{cm}^2 \text{sec}}, \quad \eta_S \simeq 0.60, \quad \tau_{diss} \simeq 8.0 \cdot 10^7 \text{ sec}, \quad \kappa \simeq 2.0 \cdot 10^{-2} \text{ sec}^{-1},
 \end{aligned}
 \tag{28}$$

Indeed, Fig. 12 shows that our light curve is able to account for the light curve of XRF 050416A.

3. ORIGIN OF GAMMA RAY BURSTS FROM P-STAR MODEL

The results in previous Section show that the light curves of Swift gamma ray bursts can be successfully described by the approach developed in Cea (2006) to quantitatively account for light curves for both soft gamma repeaters and anomalous X-ray pulsars. This leads us to suppose that the same mechanism is responsible for bursts from gamma ray bursts, soft gamma repeaters, and anomalous X-ray pulsars.

In Cea (2006) we showed that soft gamma repeaters and anomalous X-ray pulsars can be understood within our recent proposal of p-stars, namely compact quark stars in β -equilibrium with electrons in a chromomagnetic condensate (Cea 2004a,b). In particular, the bursts are powered by glitches, which in our model are triggered by dissipative effects in the inner core. The energy released during a burst is given by the magnetic energy directly injected into the magnetosphere:

$$\delta E_B^{ext} \simeq \frac{1}{3} R^3 B_S^2 \frac{\delta B_S}{B_S} . \quad (29)$$

For magnetic powered pulsars with $M \sim M_\odot$ and $R \sim 10 \text{ Km}$, we have $B_S \lesssim 10^{17} \text{ Gauss}$. So that, from Eq. (29) we get:

$$\delta E_B^{ext} \simeq 2.6 \cdot 10^{50} \text{ ergs} \left(\frac{B_S}{10^{17} \text{ Gauss}} \right)^2 \frac{\delta B_S}{B_S} \lesssim 2.6 \cdot 10^{50} \text{ ergs} . \quad (30)$$

The gamma-ray energy released in gamma ray bursts is narrowly clustered around $5.0 \cdot 10^{50} \text{ ergs}$ (Frail et al. 2001). Thus, even though it is conceivable that a small fraction of gamma ray bursts could be explained by burst like the 2004 December 27 giant flare from SGR 1806-20, we see that canonical magnetic powered pulsars (canonical magnetars) do not match the required energy budget to explain gamma ray bursts. On the other hand, we find that massive magnetars, namely magnetic powered pulsars with $M \sim 10 M_\odot$ and $R \sim 10^2 \text{ Km}$, could furnish the energy needed to fire the gamma ray bursts.

The possibility to have massive pulsars stems from the fact that our p-stars do not admit the existence of an upper limit to the mass of a completely degenerate configuration. In other words, our peculiar equation of state of degenerate up and down quarks in a chromomagnetic condensate allows the existence of finite equilibrium states for stars of arbitrary mass. In fact, in Fig. 13 we display the gravitational mass versus the radius for p-stars with chromomagnetic condensate $\sqrt{gH} = 0.1 \text{ GeV}$.

Note that the strength of the chromomagnetic condensate of massive magnetars is reduced by less than one order of magnitude with respect to canonical magnetars. Thus, we infer that for massive pulsars $B_S \lesssim 10^{16} \text{ Gauss}$. Using Eq. (29) we find:

$$\delta E_B^{ext} \simeq 2.6 \cdot 10^{51} \text{ ergs} \left(\frac{B_S}{10^{16} \text{ Gauss}} \right)^2 \frac{\delta B_S}{B_S} \lesssim 2.6 \cdot 10^{51} \text{ ergs} , \quad (31)$$

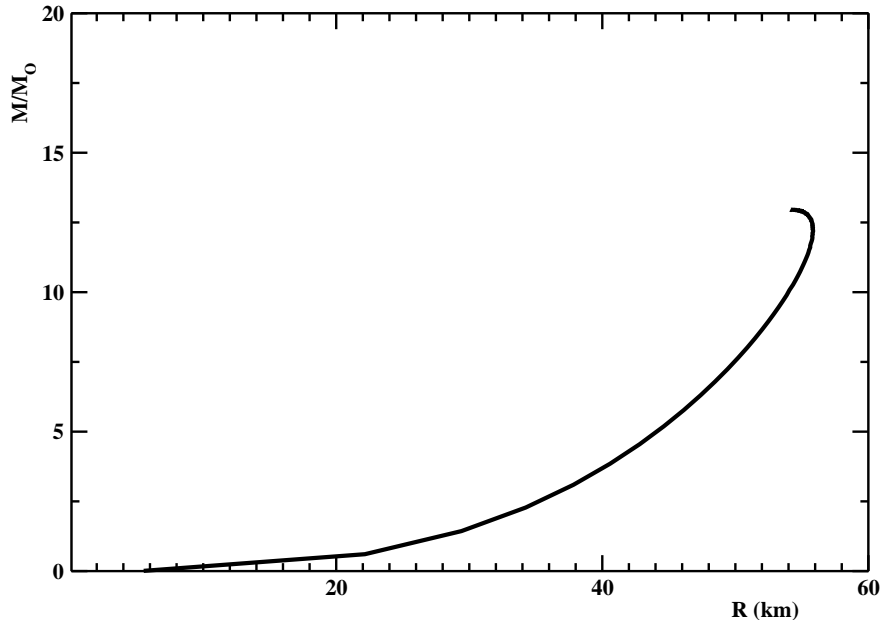


Fig. 13.— Gravitational mass M plotted versus stellar radius R for p-stars with $\sqrt{gH} = 0.1 \text{ GeV}$.

that, indeed, confirms that massive magnetars are a viable mechanism for gamma ray bursts.

An interesting consequence of our proposal is that at the onset of the bursts there is an almost spherically symmetric outflow from the pulsar, together with a collimated jet from the north magnetic pole (Cea 2006). Indeed, following the 2004 27 December giant flare from SGR 1806-20 it has been detected a radio afterglow consistent with a spherical, non relativistic expansion together with a sideways expansion of a jetted explosion. More interestingly, the lower limit of the outflow energy turns out to be $E \gtrsim 10^{44.5} \text{ ergs}$ (Gelfand et al. 2005). This implies that the blast wave and the jet may dissipate up to about 10% of the total burst energy. In the case of gamma ray bursts, according to our proposal we see that at the onset of the burst there is a matter outflow with energies up to $\sim 10^{50} \text{ ergs}$. We believe that this could explain the association of some gamma ray bursts with supernova explosions.

4. CONCLUSIONS

Let us conclude by briefly summarizing the main results of the present paper. We have presented an effective theory which allows us to account for X-ray light curves of both gamma ray bursts and X-ray rich flashes. We have shown that the approach developed to describe the light curves from anomalous X-ray pulsars and soft gamma-ray repeaters

works successfully even for gamma ray bursts. This leads us the conclusion that the same mechanism is responsible for bursts from gamma ray bursts, soft gamma repeaters, and anomalous X-ray pulsars. In fact, we propose that gamma ray bursts originate by the burst activity from massive magnetic powered pulsars.

REFERENCES

- Burrows, D.N., et al. 2006, astro-ph/0604320
- Campana, S., et al. 2006, astro-ph/0603279, accepted for publication in Nature
- Cea, P. 2004a, Int. J. Mod. Phys. D, 13, 1917
- Cea, P. 2004b, JCAP, 0403011
- Cea, P. 2006, A&A, 450, 199
- Cheng, B., Epstein, R. I., Guyer, R. A., & Cody Young, A. 1995, Nature, 382, 518
- Chincarini, G., SWIFT Collaboration 2005, astro-ph/0511108
- Cusumano, G., et al. 2006, ApJ, 639, 316
- Dado, S., Dar, A., & De Rujula, A. 2006, astro-ph/0512196
- Feroci, M., et al. 2003, ApJ, 596, 470
- Frail, D., et al. 2001, ApJ, 562, L55
- Gelfand, J.D., et al. 2005, ApJ, 634, L89
- Granot, J., Konigl, A., & Piran, T. 2006, astro-ph/0601056
- Guetta, D., et al. 2006, astro-ph/0602387
- Hurkett, C.P., et al. 2006, MNRAS, 368, 1101
- La Parola, V., et al 2006, astro-ph/0602541
- Levan, A.J., et al 2006, astro-ph/0603282
- Mangano, V., et al 2006, astro-ph/0603738
- Mészáros, P. 2006, astro-ph/0605208

Morris, D.C., et al. 2006, astro-ph/0602490

Nousek, J.A., et al. 2006, ApJ, 642, 389

O’Brien, P.T., et al. 2006, astro-ph/0601125, accepted for publication in ApJ

Piran, T. 2005, Rev. Mod. Phys. 76, 1143

Romano, P., et al. 2006a, A&A, 450, 59 %

Romano, P., et al. 2006b, astro-ph/0602497, accepted for publication in A&A

Rykoff, E.S., et al. 2006, ApJ, 638, L5

Soderberg, A.M., et al. 2006, astro-ph/0601455

Vaughan, S., et al. 2006, ApJ, 638, 920

Woods, P.M., et al. 2004, ApJ, 605, 378